

Study of Scalar Mesons at BES-II

Haibo Li^a *

^aInstitute of High Energy Physics, P.O.Box 918, Beijing 100049, China

Recent results from BES-II experiment on hadron spectroscopy using J/ψ and ψ' data samples collected in e^+e^- annihilation are presented, including study of the scalar particles in J/ψ radiative and hadronic decays, the observation of $X(1810)$ in $J/\psi \rightarrow \gamma\phi\omega$, as well as pair productions of scalars in χ_{c0} hadronic decays.

1. Introduction

The scalar mesons are one of the most controversial subjects in hadron physics. Below 1.0 GeV, there are two $I = 0$ scalar candidates, σ ($\pi\pi$ S-Wave), $f_0(980)$ and one $I = 1/2$ $K\pi$ S-wave, κ , in the Particle Data Group (PDG) lists [1]. Between 1.0 GeV and 2.2 GeV, PDG lists the following $I = 0$ scalar states: $f_0(1370)$, $f_0(1500)$, $f_0(1710)$ and one $I = 1/2$ scalar state: $K_0^*(1430)$. Scalar mesons have been traditionally studied in scattering experiments. However, in these experiments the mesons can be difficult to disentangle from non-resonant backgrounds. Radiative and hadronic J/ψ decays provide an excellent laboratory to probe these states.

Recently, based on 58 million J/ψ decay events and 14 million $\psi(2S)$ decay events collected with BES-II detector [2], many detailed partial wave analyses (PWA) have been performed in order to understand the structure, decays and production of the scalar mesons. In this paper, we present some of the results from such study at BES-II.

2. Scalars in J/ψ Radiative and Hadronic Decays

Using the world largest J/ψ data sample in e^+e^- annihilation experiment, BES-II studied the scalars decay into pair of pseudoscalars ($\pi^+\pi^-$, $\pi^0\pi^0$, K^+K^- and $K_s^0K_s^0$) in J/ψ radiative decays as well as recoiling against a ϕ or an ω [3,4,5,6]. The full mass spectra and the scalar part in them are shown in Fig. 1.

2.1. σ and κ

From the analyses, BES-II sees significant contributions of σ particle in $\omega\pi^+\pi^-$ and ωK^+K^- , and also hint in $\phi\pi^+\pi^-$. In $J/\psi \rightarrow \omega\pi^+\pi^-$, there are conspicuous $\omega f_2(1270)$ and $b_1(1235)\pi$ signals. At low $\pi\pi$ mass, a large, broad peak due to the σ is observed as shown in Fig. 1(a). Two independent partial wave analyses are performed on $\omega\pi^+\pi^-$ data and four different parameterizations of the σ amplitude are tried [3], all give consistent results for the σ pole, which is at $(541 \pm 39) - i(252 \pm 42)$ MeV/ c^2 . Recently, an analysis of $\psi(2S) \rightarrow \pi^+\pi^- J/\psi$ has been performed to study the σ [7]. The pole position of σ is consistent with that from $J/\psi \rightarrow \omega\pi^+\pi^-$.

Events over all of the 4-body phase space for $J/\psi \rightarrow K^+K^-\pi^+\pi^-$ have been fitted. We find evidence for the κ in the process $J/\psi \rightarrow \bar{K}^*(892)^0\kappa$, $\kappa \rightarrow (K\pi)_S$. We select a $K^-\pi^+$ pair in the $\bar{K}^*(892)^0$ mass range 892 ± 100 MeV. Two independent PWA, by the covariant helicity amplitude method [8] and by the variant mass and width method [9] have been performed, providing a cross check with each other. They reproduce the data well, and the results are in good agreement. The low mass enhancement is well described by the scalar κ , which is highly required in the analyses. Parameter values of Breit-Wigner (BW) mass and width of the κ , averaged from those obtained by the two methods, are $878 \pm 23_{-55}^{+64}$ MeV/ c^2 and $499 \pm 52_{-87}^{+55}$ MeV/ c^2 . The pole position is determined to be $(841 \pm 30_{-73}^{+81}) - i(309 \pm 45_{-72}^{+48})$ MeV/ c^2 [10].

*Email: lihb@ihep.ac.cn

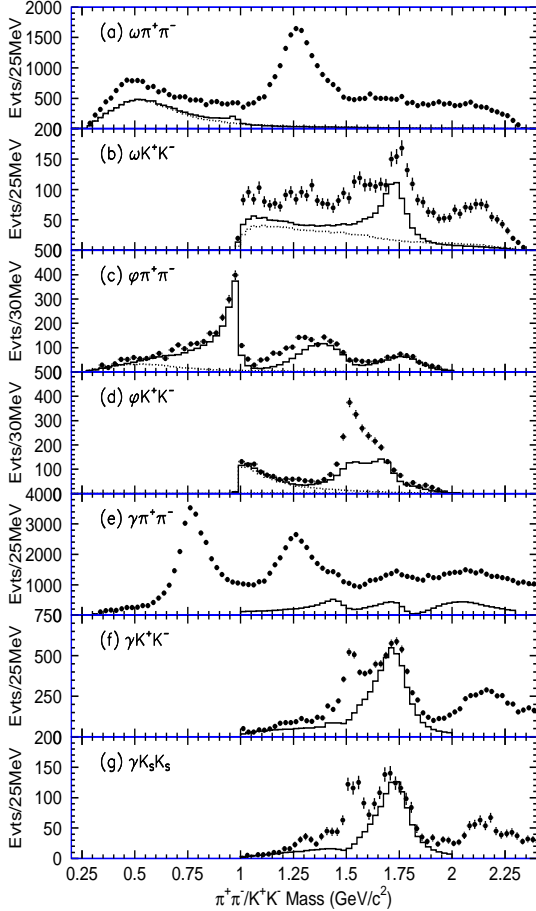


Figure 1. The invariant mass distributions of the pseudoscalar meson pairs recoiling against ω , ϕ , or γ in J/ψ decays measured at BES-II. The dots with error bars are data, the solid histograms are the scalar contribution from PWA, and the dashed lines in (a) through (c) are contributions of σ from the fits, while the dashed line in (d) is the $f_0(980)$. Notice that not the full mass spectra are analyzed in (e), (f), and (g). Results in (e) are preliminary, otherwise are published

2.2. $f_0(980)$ in J/ψ Decays

Strong $f_0(980)$ is seen in $J/\psi \rightarrow \phi\pi^+\pi^-$ and ϕK^+K^- modes [5], from which the resonance parameters are measured to be $M = 965 \pm 8(stat) \pm 6(syst) \text{ MeV}/c^2$, $g_1 = 165 \pm 10(stat) \pm 15(syst) \text{ MeV}/c^2$ and $g_2/g_1 = 4.21 \pm 0.25(stat) \pm 0.21(syst)$, where M is the mass, and g_1 and g_2 are the couplings to $\pi\pi$ and $K\bar{K}$ respectively if the $f_0(980)$ is parameterized using the the Flatté's formula. The production of $f_0(980)$ is very weak recoiling against an ω or a photon, which indicates $s\bar{s}$ is the dominant component in it.

2.3. Scalar above 1.0 GeV in J/ψ Decays

In $J/\psi \rightarrow \phi\pi^+\pi^-$ decay, a scalar contribution near 1.4 GeV on $\pi^+\pi^-$ invariant mass distribution is found as shown in Fig. refscalars(c), it is due to the dominant $f_0(1370)$ interfering with a smaller $f_0(1500)$ component. The mass and width of $f_0(1370)$ are determined to be: $M = 1350 \pm 50 \text{ MeV}/c^2$ and $\Gamma = 265 \pm 40 \text{ MeV}/c^2$. In $\gamma\pi^+\pi^-$, a similar structure is observed in the same mass region, the fit yields a resonance at mass $1466 \pm 6(stat) \pm 16(syst) \text{ MeV}/c^2$ with width of $108_{-11}^{+14}(stat) \pm 21(syst) \text{ MeV}/c^2$, possibly the $f_0(1500)$ [5], and the contribution from the $f_0(1370)$ can not be excluded. While, the production of $f_0(1370)$ and $f_0(1500)$ in $\gamma K\bar{K}$ is insignificant [6].

The K^+K^- invariant mass distributions from $\gamma K\bar{K}$ and ωK^+K^- , the $\pi^+\pi^-$ invariant mass distributions from $\gamma\pi^+\pi^-$, and $\phi\pi^+\pi^-$ show clear scalar contribution around $1.75 \text{ GeV}/c^2$. Two states are resolved from the bump, one is $f_0(1710)$ with $M \sim 1740 \text{ MeV}/c^2$ and $\Gamma \sim 150 \text{ MeV}/c^2$ which decays to $K\bar{K}$ mostly, and one possible new state $f_0(1790)$ with $M \sim 1790 \text{ MeV}/c^2$ and $\Gamma \sim 270 \text{ MeV}/c^2$ which couples to $\pi\pi$ stronger than to $K\bar{K}$. However, the existence of the second scalar particle needs confirmation: the signal observed in $\phi f_0(1790)$ is rather in the edge of the phase space, and the reconstruction efficiency of the ϕ decreases dramatically as the momentum of the ϕ decreases thus the momentum of the kaon from ϕ decays is very low and can not be detected [7]. Furthermore, there are wide higher mass scalar states above $2 \text{ GeV}/c^2$ as observed in

$\gamma\pi^+\pi^-$ (Fig. 1e) and $\gamma K\bar{K}$ [1], whose tails may interfere with the $f_0(1710)$ and produce structure near the edge of the phase space.

The discussions of these measurements for understanding the nature of the scalar particles can be found in Refs. [11,12,13], where the J/ψ decay dynamics and the fractions of the possible $q\bar{q}$ and glueball components in the states are examined.

3. Observation of Threshold Enhancements in J/ψ Decays

In the last few years, anomalous enhancements near threshold in the invariant mass spectra of $p\bar{p}$ and $p\bar{\Lambda}$ pairs were observed in $J/\psi \rightarrow \gamma p\bar{p}$ [14] and $J/\psi \rightarrow pK\bar{\Lambda}$ [15] decays, respectively, by the BES-II experiment. These surprising experimental observations stimulated many theoretical speculations. Therefore it is of special interests to search for possible resonances in other baryon-antibaryon, baryon-meson, and meson-meson final states.

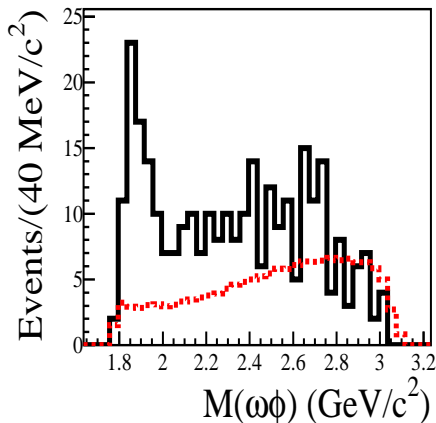


Figure 2. The $K^+K^-\pi^+\pi^-\pi^0$ invariant mass distribution for the $J/\psi \rightarrow \gamma\omega\phi$ candidate events. The dashed curve indicates the acceptance varying with the $\omega\phi$ invariant mass.

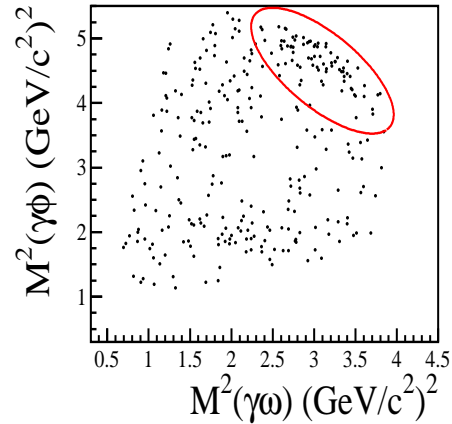


Figure 3. $M^2(\gamma\phi)$ vs. $M^2(\gamma\omega)$, Dalitz plot in $J/\psi \rightarrow \gamma\phi\omega$ decay.

3.1. $X(1810)$ in $J/\psi \rightarrow \gamma\phi\omega$ Decays

An enhancement near threshold is observed in the $\omega\phi$ invariant mass spectrum from the doubly OZI suppressed decays of $J/\psi \rightarrow \gamma\omega\phi$, where ω and ϕ are reconstructed from $\pi^+\pi^-\pi^0$ and K^+K^- final states [16], respectively. Figure 2 shows the $K^+K^-\pi^+\pi^-\pi^0$ invariant mass distribution for events with K^+K^- invariant mass within the nominal ϕ mass range ($|m_{K^+K^-} - m_\phi| < 15 \text{ MeV}/c^2$) and the $\pi^+\pi^-\pi^0$ mass within the ω mass range ($|m_{\pi^+\pi^-\pi^0} - m_\omega| < 30 \text{ MeV}/c^2$), and a structure peaked near $\omega\phi$ threshold is observed. The dashed curve in the figure indicates how the acceptance varies with invariant mass. The peak is also evident as a diagonal band along the upper right-hand edge of the Dalitz plot in Fig. 3. There is also a horizontal band near $m_{\gamma K^+K^-}^2 = 2 \text{ (GeV}/c^2)^2$ in the Dalitz plot, which mainly comes from background due to $J/\psi \rightarrow \omega K^*K$.

From a PWA with covariant helicity coupling amplitudes, the spin-parity of the $X = 0^{++}$ with an \mathcal{S} -wave $\omega\phi$ system is favored. The enhancement near is observed with a statistical significance of more than 10σ . The mass and width of the enhancement are determined to be $M =$

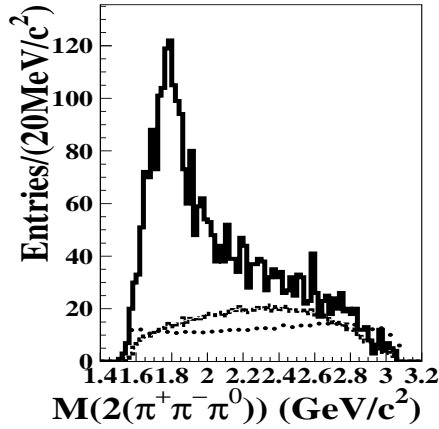


Figure 4. The $2(\pi^+\pi^-\pi^0)$ invariant mass distribution for candidate events. The dashed curve is the phase space invariant mass distribution, and the dotted curve shows the acceptance versus the $\omega\omega$ invariant mass.

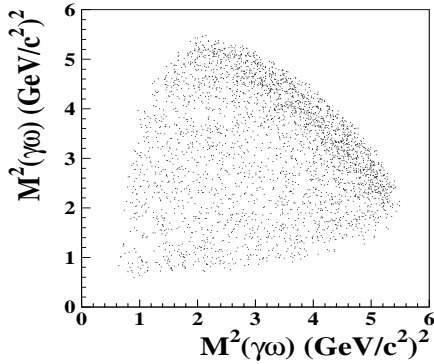


Figure 5. The Dalitz plot in $J/\psi \rightarrow \gamma\omega\omega$ decays.

1812_{-26}^{+19} (stat) ± 18 (syst) MeV/c^2 and $\Gamma = 105 \pm 20$ (stat) ± 28 (syst) MeV/c^2 , and the product branching fraction is $\mathcal{B}(J/\psi \rightarrow \gamma X) \cdot \mathcal{B}(X \rightarrow \omega\phi) = (2.61 \pm 0.27$ (stat) ± 0.65 (syst)) $\times 10^{-4}$. The mass and width of this state are not compatible with any known scalars listed in the PDG [1]. It could be an unconventional state [17,18,19,20,21]. However, more statistics and further studies are needed to clarify this.

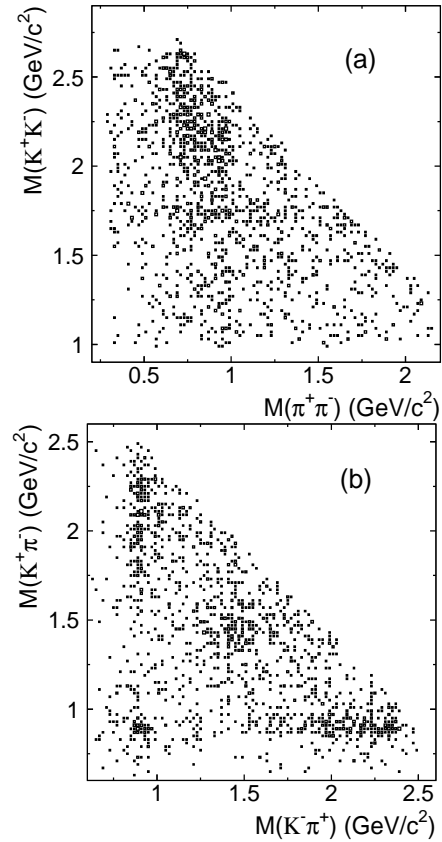


Figure 6. The scatter plots of (a) K^+K^- versus $\pi^+\pi^-$ and (b) $K^+\pi^-$ versus $K^-\pi^+$ invariant mass for selected $\psi' \rightarrow \gamma\chi_{c0}$, $\chi_{c0} \rightarrow \pi^+\pi^-K^+K^-$ events.

Table 1

Summary of the $\chi_{c0} \rightarrow \pi^+\pi^-K^+K^-$ results, where X represents the intermediate decay modes, N^{obs} is the number of fitted events, and s.s. indicates signal significance.

Decay Mode (X)	N^{obs}	$\mathcal{BR}(10^{-4})$ $\mathcal{BR}(\chi_{c0} \rightarrow X \rightarrow \pi^+\pi^-K^+K^-)$	s.s
$f_0(980)f_0(980)$	27.9 ± 8.7	$3.46 \pm 1.08^{+1.93}_{-1.57}$	5.3σ
$f_0(980)f_0(2200)$	77.1 ± 13.0	$8.42 \pm 1.42^{+1.65}_{-2.29}$	7.1σ
$f_0(1370)f_0(1710)$	60.6 ± 15.7	$7.12 \pm 1.85^{+3.28}_{-1.68}$	6.5σ
$K^*(892)^0\bar{K}^*(892)^0$	64.5 ± 13.5	$8.09 \pm 1.69^{+2.29}_{-1.99}$	7.1σ
$K_0^*(1430)\bar{K}_0^*(1430)$	82.9 ± 18.8	$10.44 \pm 2.37^{+3.05}_{-1.90}$	7.2σ
$K_0^*(1430)\bar{K}_2^*(1430) + c.c.$	62.0 ± 12.1	$8.49 \pm 1.66^{+1.32}_{-1.99}$	8.7σ
$K_1(1270)^+K^- + c.c.$, $K_1(1270) \rightarrow K\rho(770)$	68.3 ± 13.4	$9.32 \pm 1.83^{+1.81}_{-1.64}$	8.6σ
$K_1(1400)^+K^- + c.c.$, $K_1(1400) \rightarrow K^*(892)\pi$	19.7 ± 8.9	< 11.9 (90% C.L.)	2.7σ

3.2. Enhancement in $J/\psi \rightarrow \gamma\omega\omega$ Decays

The decay mode $J/\psi \rightarrow \gamma\omega\omega$, $\omega \rightarrow \pi^+\pi^-\pi^0$ is analyzed using a sample of 5.8 million J/ψ decay events. The $\omega\omega$ invariant mass distribution peaks at $1.76 \text{ GeV}/c^2$, just above the $\omega\omega$ threshold. The histogram of Fig. 4 shows the $2(\pi^+\pi^-\pi^0)$ invariant mass distribution of events with both $\pi^+\pi^-\pi^0$ masses within the ω range ($|m_{\pi^+\pi^-\pi^0} - m_\omega| < 40 \text{ MeV}/c^2$). There are 3046 events with a clear peak at $1.76 \text{ GeV}/c^2$. The phase space invariant mass distribution and the acceptance versus $\omega\omega$ invariant mass are also shown in the figure. The corresponding Dalitz plot is shown in Fig. 5.

The partial wave analysis shows a strong contribution from 0^- for the $\omega\omega$ invariant mass below $2.0 \text{ GeV}/c^2$, and with small contributions from $f_0(1710)$, $f_2(1640)$, and $f_2(1910)$. Therefore the study of the $\eta(1760)$ is the main goal of this analysis. The mass of the pseudoscalar is $M = 1744 \pm 10$ (stat) ± 15 (syst) MeV/c^2 , the width $\Gamma = 244^{+24}_{-21}$ (stat) ± 25 (syst) MeV/c^2 , and the product branching fraction is $\text{Br}(J/\psi \rightarrow \gamma\eta(1760)) \cdot \text{Br}(\eta(1760) \rightarrow \omega\omega) = (1.98 \pm 0.08$ (stat) ± 0.32 (syst)) $\times 10^{-3}$.

4. Pair Productions of Scalars in $\chi_{c0} \rightarrow \pi^+\pi^-K^+K^-$

PWA of $\chi_{c0} \rightarrow \pi^+\pi^-K^+K^-$ is performed [22] using χ_{c0} produced in ψ' decays at BES-II. In 14 M produced ψ' events, 1371 $\psi' \rightarrow \gamma\chi_{c0}$, $\chi_{c0} \rightarrow$

$\pi^+\pi^-K^+K^-$ candidates are selected with around 3% background contamination.

Figure 6(a) shows the scatter plot of K^+K^- versus $\pi^+\pi^-$ invariant mass which provides further information on the intermediate resonant decay modes for $(\pi^+\pi^-)(K^+K^-)$ decay, while Fig. 6(b) shows the scatter plot of $K^+\pi^-$ versus $K^-\pi^+$ invariant masses for the resonances with strange quark.

Besides $(\pi\pi)(KK)$ and $(K\pi)(K\pi)$ modes, $(K\pi\pi)K$ mode which leads to a measurement of $K_1(1270)K$ and $K_1(1400)K$ decay processes is also included in the fit. The PWA results are summarized in Table 1. From these results, we notice that scalar resonances have larger decay fractions compared to those of tensors, and such decays provide a relatively clean laboratory to study the properties of scalars, such as $f_0(980)$, $f_0(1370)$, $f_0(1710)$, and so on.

The above results supply important information on the understanding of the natures of the scalar states [23].

REFERENCES

1. S. Eidelman *et al.*, Phys. Lett. **B592** (2004) 1.
2. BES Collaboration, J. Z. Bai *et al.*, Nucl. Inst. Meth. **A458** (2001) 627.
3. BES Collaboration, M. Ablikim *et al.*, Phys. Lett. B **598**, 149 (2004).

4. BES Collaboration, M. Ablikim *et al.*, Phys. Lett. B **603** (2004) 138.
5. BES Collaboration, M. Ablikim *et al.*, Phys. Lett. B **607** (2004) 243.
6. BES Collaboration, J. Z. Bai *et al.*, Phys. Rev. D **68**, (2003) 052003.
7. C. Z. Yuan, hep-ex/0510062.
8. N. Wu and T. N. Ruan, Commun. Theor. Phys. (Beijing, China) **35** (2001) 547; N. Wu and T. N. Ruan, Commun. Theor. Phys. (Beijing, China) **35** (2001) 693; N. Wu and T. N. Ruan, Commun. Theor. Phys. (Beijing, China) **37** (2002) 309.
9. S. Ishida *et al.*, Prog. Theor. Phys. **95** (1996) 745;
10. BES Collaboration, M. Ablikim *et al.*, Phys. Lett. B **633** (2006) 681.
11. L. Roca *et al.*, Nucl. Phys. A **744** (2004) 127.
12. F. Close and Q. Zhao, Phys. Rev. **D71** (2005) 094022.
13. Q. Zhao, B.S. Zou and Z.B. Ma, Phys. Lett. **B631** (2005) 22.
14. BES Collaboration, J.Z. Bai *et al.*, Phys. Rev. Lett. **91** (2003) 022001.
15. BES Collaboration, M. Ablikim *et al.*, Phys. Rev. Lett. **93** (2004) 112002.
16. BES Collaboration, M. Ablikim *et al.*, hep-ex/0602031, accepted by Phys. Rev. Lett..
17. Bing An Li, hep-ph/0602072
18. Xiao-Gang He, Xue-Qian Li *et al.*, Phys. Rev. D **73** (2006) 051502.
19. Pedro Bicudo *et al.*, hep-ph/0602172 .
20. Kuang-Ta Chao, hep-ph/0602190.
21. D.V. Bugg, hep-ph/0603018.
22. BES Collaboration, M. Ablikim, *et al.*, Phys. Rev. **D72** (2005) 092002.
23. Q. Zhao, Phys. Rev. **D72** (2005) 074001